JOURNAL OF SPACECRAFT AND ROCKETS
Vol. 53, No. 4, July-August 2016

Engineering Notes

Technique to Optimize for Engine Shutoff Constraints in Electric-Propulsion Trajectories

Jason A. Reiter* and David B. Spencer†
Pennsylvania State University, University Park, Pennsylvania 16802

DOI: 10.2514/1.A33397

Nomenclature

a	=	semimajor axis, km
E	=	eccentric anomaly, rad
e	=	eccentricity
f	=	acceleration magnitude due to thrust on the spacecraft, m/s^2
i	=	inclination, rad
p	=	semilatus rectum, km
r	=	distance from the spacecraft to the central body, km
$\boldsymbol{T}$	=	thrusting vector angle, N
u	=	true latitude, rad
w_{eff}	=	efficiency-based weighting
w_{position}	=	position-based weighting
α	=	in-plane thrusting angle, rad
β	=	out-of-plane thrusting angle, rad
η	=	maneuver efficiency
ν	=	true anomaly, rad
Ω	=	right ascension of the ascending node, rad
ω	=	argument of perigee, rad

I. Introduction

MANY techniques exist for solving electric-propulsion trajectories. Ever since the inclined circular orbit transfer was first optimized by Edelbaum in Chobotov [1], advances in the optimization of low-thrust orbit transfers have been ongoing. Kechichian in Conway [2] expanded on Edelbaum's work to constrain the intermediate orbits during the transfer to remain below a given altitude and reformulated the problem within the framework of optimal control theory while applying analytic averaging. Kluever [3] then modified Kechichian's work to allow for the inclusion of shutoffs due to eclipse periods. Additional advances have been made in optimizing low-thrust orbit transfers, including Q-law, nonlinear programming, and indirect optimization. Though these techniques can provide highly optimal propellant versus time curves, the nature of these techniques only allows for eclipse periods to be incorporated as unplanned shutoffs [4]. Although optimal control, such as in Kluever's work [3], can account for eclipse periods and other arbitrary engine shutoff periods, only the time-optimal solution can be found with this method. Feedback control, however, allows for an optimization (minimizing the fuel use and time-of-flight simultaneously) of the trajectory, including the effects of shutoff periods, while creating a complete propellant versus time curve [5].

With techniques that cannot optimize maneuvers around required engine shutoffs, eclipse periods are accounted for simply as unplanned shutoffs. When creating a propellant versus time curve using these techniques, propellant use is lowered by simply taking more time and only thrusting when it is most efficient to do so. If an unplanned shutoff were to occur during the small amount of time planned for thrusting, this would mean a large increase in flight time, if the transfer solution converges at all. The goal of this paper is to develop a forward-looking feedback control method that can be used to plan engine shutoff periods and therefore optimize an orbit transfer. The feedback method simplifies the problem and improves both the convergence properties and the robustness for such scenarios. For example, if eclipse periods occur when thrusting is most efficient, then the forward-looking feedback method will call for thrusting at slightly less efficient points to ensure that the transfer is still completed in a realistic time frame. This ability to optimize around eclipse periods means much more realistic time-of-flight and fuel use estimates for solar powered low-thrust transfers and may prove useful in applying similar methods in future work.

II. Methodology

The main concept behind this technique is the use of feedback control based on the proximity of the spacecraft to its desired end state. With an initial state and desired end state, the optimal thrusting angle can be calculated throughout the trajectory to reach the desired end state. Applying directionality and efficiency thresholds also allows for an increase in propellant usage efficiency at the expense of a longer flight time [5].

A. Approach

In [6], a feedback control law (restated in Table 1) is described, in which the optimal angle to increase each classical orbital element (COE) is weighted based on the COE's relative distance from its end state. The weighted angles are then combined so that the spacecraft is thrusting in the optimal direction for all desired COEs to reach their end states simultaneously. A threshold is then applied so that thrusting does not occur at points where it is inefficient to do so.

Using this control law as a basis, changes are made to maximize the effect of the controller. In addition to the location-based weighting, a second weighting is applied to the angle based on the instantaneous maneuver efficiency. An additional threshold is also applied to account for conflicting optimal thrusting directions. The optimal thrusting angle is updated at each time step, and the efficiency and thrusting direction are compared to the user-designated cutoff thresholds. If the thresholds are not met, thrusting does not occur. Applying a range of efficiency thresholds allows for a curve to be constructed comparing propellant mass use and maneuver time.

B. Propagation Method

To save computation time (compared to MATLAB's ode45) and avoid convergence tolerance issues, the COE differential equations presented in [6] are combined with Euler's method to propagate the orbital states. The differential equations for the semimajor axis, eccentricity, inclination, right ascension of the ascending node, and argument of perigee are

Received 18 July 2015; revision received 28 February 2016; accepted for publication 4 April 2016; published online 6 June 2016.

*Graduate Research Assistant, Department of Aerospace Engineering, 229 Hammond Building. Student Member AIAA.

†Professor, Department of Aerospace Engineering, 229 Hammond Building. Associate Fellow AIAA.

$$\frac{\mathrm{d}a}{\mathrm{d}t} = \frac{2a^2}{h} f \cos\beta \left\{ e \sin\nu \sin\alpha + \frac{p}{r} \cos\alpha \right\} \tag{1}$$

$$\frac{\mathrm{d}e}{\mathrm{d}t} = \frac{1}{h} f \cos\beta \{ p \sin\nu \sin\alpha + ((p+r)\cos\nu + re)\cos\alpha \} \tag{2}$$

$$\frac{\mathrm{d}i}{\mathrm{d}t} = f \frac{r}{h} \cos u \sin\beta \tag{3}$$

$$\frac{\mathrm{d}\Omega}{\mathrm{d}t} = f \frac{r}{h} \frac{\sin u}{\sin i} \sin\beta \tag{4}$$

$$\frac{\mathrm{d}\omega}{\mathrm{d}t} = \frac{1}{he} f \cos\beta \{ -p \cos\nu \sin\alpha + (p+r)\sin\nu \cos\alpha \} - f \frac{r \sin u \cos i}{h \sin i} \sin\beta \tag{5}$$

C. Control Law

The thrust direction angles are solved for each COE separately using the equations in Table 1. These are the in-plane (α) and out-of-plane (β) thrusting angles, both measured from the circumferential direction in the radial–circumferential–normal (RCN) reference frame, for the maximum instantaneous time rate of change of each orbital element, regardless of their effect on the other orbital elements.

When more than one COE is changed in the orbital maneuver, the separate angles are combined together to make one optimal vector of angles α and β. To do this, the angles must first be transformed into the body-fixed radial–circumferential–normal (RCN) reference frame. This reference is such that the radial component is aligned with the radial unit vector positive in the zenith direction, the normal component is aligned with the osculating angular momentum vector positive in the direction of the cross product $\boldsymbol{R} \times \boldsymbol{V}$, and the circumferential component is normal to the radius vector in the orbital plane and completes the right-handed triad of unit vectors. The transformation from α and β to RCN can be calculated for each COE:

$$\boldsymbol{T}_{\mathrm{COE}} = [\sin\alpha \cos\beta, \cos\alpha \cos\beta, \sin\beta]^T \tag{6}$$

Two weightings are applied to this vector. The first is based on the relative value for the COE compared to its starting state and desired final state to ensure that all orbital elements converge simultaneously:

$$w_{\mathrm{position}} = \frac{z_1 - z}{|z_1 - z_0|} \tag{7}$$

where z_1 is the desired final value, z is the instantaneous osculating value, and z_0 is the starting value for each COE being controlled. The second weighting is calculated using the instantaneous maneuver efficiency of each COE, defined as the relative time rate of change at which the desired COE can be increased or decreased. As expected, the efficiency to change each orbital element varies throughout a single revolution. Table 2 [6] summarizes the locations (true anomaly) of the maximum instantaneous efficiency for each COE and the equations for the instantaneous efficiency at any true anomaly value, found by taking the derivative of Eqs. (1–5) with respect to time and dividing by the same equation evaluated at the location of maximum efficiency.

Using the equations for instantaneous maneuver efficiency η, the second weighting is found by dividing the instantaneous efficiency for the COE by the average maneuver efficiency for that COE over one revolution:

$$w_{\mathrm{eff}} = \frac{\eta_z}{\int_0^{2\pi} \eta_z(\nu)\,\mathrm{d}\nu} \tag{8}$$

The two weights are then multiplied by the optimal thrusting vector for the corresponding COE, and the resulting vectors for all controlled COEs are added together to get a single optimal instantaneous thrusting angle"

$$\boldsymbol{T} = \sum_z w_{\mathrm{eff}} w_{\mathrm{position}} \boldsymbol{T}_{\mathrm{COE}} \tag{9}$$

where Σ_z signifies the summation of the term for all controlled COEs. This vector is then transformed back into angles α (the inverse tangent of the radial magnitude of the angle $\boldsymbol{T}_R$ divided by the circumferential magnitude $\boldsymbol{T}_C$) and β (the inverse tangent of the normal magnitude of the angle $\boldsymbol{T}_N$) divided by the hypotenuse of the triangle created by connecting the normal and circumferential vectors ($\sqrt{\boldsymbol{T}_R^2 + \boldsymbol{T}_C^2}$), which are inserted into Eqs. (1–5) to propagate the transfer at each time step.

Table 1 Optimal thrust angles for the maximum instantaneous change of each orbital element

Classic orbital element	In-plane angle, rad	Out-of-plane angle, rad
Semi-major axis a	$\alpha = \tan^{-1}(e \sin\nu / 1 + e \cos\nu)$	$\beta = 0$
Eccentricity e	$\alpha = \tan^{-1}(\sin\nu / \cos\nu + \cos E)$	$\beta = 0$
Inclination i	$\alpha = 0$	$\beta = \mathrm{sgn}(\cos u)\pi/2$
Right Ascension of the Ascending Node Ω	$\alpha = 0$	$\beta = \mathrm{sgn}(\sin u)\pi/2$
Argument of perigee (ω)	$\alpha = \tan^{-1}((1 + e\cos\nu/2 + e\cos\nu)\cot\nu)$ $\beta = \tan^{-1}(e \cot i \sin u / \sin(\alpha - \nu)$ $\times(1 + e\cos\nu - \cos\alpha \sin\nu)$	

Table 2 Location of maximum rate of change, the maneuver efficiency for each COE

Classic orbital element	$\nu_{\max}$	η
a	$\nu_a = 0$	$\eta_a = V\sqrt{(a/\mu)(1 - e/1 + e)}$
e	$\nu_e = \pi$	$\eta_e = (1/2)1 + 2e\cos\nu + \cos^2\nu / 1 + e\cos\nu)$
i	$\sin(\nu_i + \omega) = -e \sin\omega$	$\eta_i = \lvert\cos(\omega + \nu)\rvert / 1 + e\cos\nu(\sqrt{1 - e^2\sin^2\omega} - e\lvert\cos\omega\rvert)$
Ω	$\cos(\nu_\Omega + \omega) = -e\cos\omega$	$\eta_\Omega = \lvert\sin(\omega + \nu)\rvert / 1 + e\cos\nu(\sqrt{1 - e^2\cos^2\omega} - e\lvert\sin\omega\rvert)$
ω	$\cos\nu_\omega = [1 - e^2/e^3 + \sqrt{(1/4)(1 - e^2/e^3)} + 1/27]^{1/3} - [-1 - e^2/e^3 + \sqrt{(1/4)(1 - e^2/e^3)} + 1/27]^{1/3} - 1/e$	$\eta_\omega = (1/4)(1 + \sin^2\nu / 1 + e\cos\nu)(1 + e\cos\nu^\omega_{\max} / 1 + \sin^2\nu^\omega_{\max})$

D. Applying Cutoff Thresholds

With the control law and propagation method in place, it is possible to get converging solutions to the desired orbit transfers. However, the controller is not performing as optimally as it could be when compared to the results of other methods, such as Q-law. Applying two cutoff thresholds improves the ability of the tool to minimize the fuel use and time-of-flight simultaneously. The first threshold is based on maneuver efficiency and builds on the approach applied in [6], where the instantaneous efficiency for each COE is compared directly to a cutoff efficiency. However, this does not ensure that applying a cutoff actually eliminates thrusting in a section of the orbit. This direct method can be improved on by instead applying a cutoff where the instantaneous efficiency for each COE is weighted by the average efficiency for the COE for one revolution, similar to the weighting system used in the feedback algorithm described previously. These weightings for each COE are summed together and divided by the total number of COEs being controlled and are then compared to a threshold (an input chosen based on the COEs being changed), which is adjusted using a cumulative distribution function for the instantaneous efficiencies over one revolution:

$$\frac{\sum_z \eta_z / \int_0^{2\pi} \eta_z(\nu)\,\mathrm{d}\nu}{\text{Number of COEs controlled}} < \text{Adjusted threshold} \tag{10}$$

where z represents each classical orbital element. Using the weighting system combined with the cumulative distribution function means that, no matter what cutoff value the user inputs, it will cut off the inefficient parts of the trajectory. The cumulative distribution function was chosen to produce more meaningful results. For example, if a cutoff threshold of 60% is chosen, then thrusting will only occur in the most efficient 40% of the orbit. Although either the direct or indirect methods can be used, the latter is recommended for more meaningful results.

This threshold method is also extremely versatile. Because the instantaneous value compared to the threshold is dependent on the average efficiency of the orbital elements, the value can be adjusted for any possible periods where thrusting is prohibited. Adding constraints on thrusting locations based on eclipse periods and mission pointing requirements (thus preventing the solar arrays from collecting energy) is straightforward and is reflected in the threshold calculation. If, for example, an eclipse occurred at a point in the orbit where it is very efficient to thrust, the average maneuver efficiency value of available locations to thrust would be lower, and so locations with lower instantaneous efficiency values would be weighted more heavily and chosen to meet the input threshold.

The second cutoff threshold is based on directionality. For certain orbital maneuvers, the combination of COEs being adjusted means that, at times, they will conflict in their optimal thrusting directions. When the conflict occurs, the resulting thrusting vector will not be ideal for reaching the desired final state because it harms the progress of one element at the expense of another. To avoid this, a threshold is applied to ensure that thrusting only occurs when it is ideal to do so. The directionality value is found from the instantaneous weighted thrusting angle for each COE by normalizing the total of all angle vectors and dividing that by the sum of each angle vector normalized:

$$\frac{\|\sum_i \boldsymbol{T}\|}{\sum_i \|\boldsymbol{T}\|} < \text{directionality} \tag{11}$$

This results in a value between zero and 1. Unlike the efficiency threshold, however, choosing a directionality threshold value (as it is an input to the tool) is not straightforward. The optimal directionality threshold varies from case to case, and in some cases, there is such thing as a bad input. For example, if the threshold is set above 0.7071, calculated from Eq. (11) assuming that the two angle vectors are [0, 1] and [1, 0], thrusting for perpendicular vectors of equal length cannot occur. This means that, with a threshold above 0.7071, it would be impossible to increase both inclination and semimajor axis/eccentricity at the same time because there is a 90 deg angle between the two vectors. However, if only in-plane thrusting is required, this would not be an issue, and values about 0.7071 could be chosen. The same method can be applied to show how the directionality threshold serves its purpose. If two COEs require thrusting in opposite directions (assuming two angle vectors of [0.8, 0] and [−0.5, 0]), the directionality value becomes small (0.2308) and easily caught by a cutoff threshold.

After applying the efficiency-based weighting to the control law and modifying the thrust locations using the two cutoff thresholds, the solutions found without including eclipse periods fit closely to results from Q-law, nonlinear programming, and indirect optimization techniques under similar conditions (as seen plotted in [5] and in Fig. 1). This test case was run with the initial and final COEs seen in Table 3 for a 2000 kg mass, 2000 s specific impulse (I_{sp}) spacecraft with 0.35 N of thrust. Comparing the results from the different tools, the modified feedback control method varies from the most robust of the state-of-the-art methods by less than a 5% error. This small error is only because techniques like the T3D averaged method apply a global optimization technique, which this method currently lacks. However, the modified feedback control method sees a significant improvement in computation time, finding each solution in mere minutes (less for smaller orbit changes) compared to hours of computation time for more robust methods. This significant decrease in computation time easily justifies a 5% error for use in preliminary mission design.

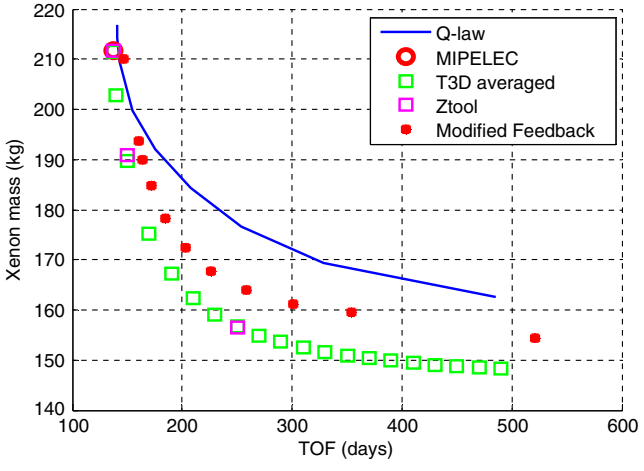

Fig. 1 Propellant mass consumption vs maneuver time for various tools.

Table 3 Initial and final COEs for the transfer scenario

Classic orbital element	Initial state	Desired final state
a, km	24, 505.9	42, 165
e	0.725	0.001
i, deg	7.05	0.05
Ω	0 deg	Free
ω	0 deg	Free

III. Results

A. Accounting for Shutoff Periods

As mentioned earlier, when applying the efficiency weighting and threshold, average efficiency values are found looking forward over one whole revolution. The ability to do this is what allows for eclipse periods to be taken into account. With a function to find the locations in the orbit where eclipsing occurs (as described by Vallado [7]), the eclipse locations can be assumed to have an efficiency of zero when calculating the average efficiency over the orbit. As seen comparing Figs. 2a and 2b, assuming the eclipse is centered at perigee (one of the most efficient points to thrust) for a semimajor axis, eccentricity, and inclination-changing maneuver, this results in a lower average efficiency value for the orbit than when the eclipse is not factored in. When finding the instantaneous efficiency (for all three COEs combined) relative to the average value and comparing it to the

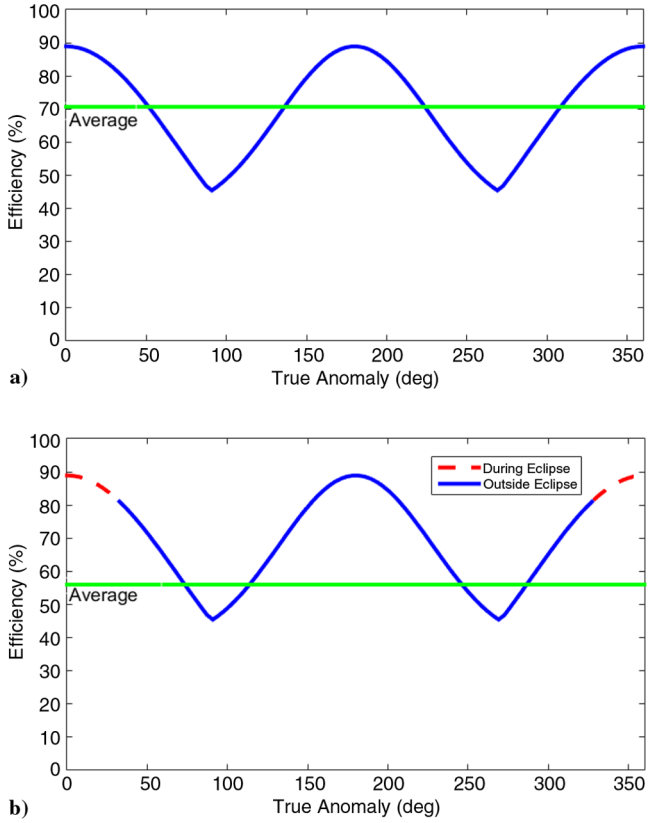

Fig. 2 Representations of instantaneous and average efficiency a) without eclipse periods and b) with eclipse periods.

desired efficiency threshold, this adjustment allows for thrusting at less efficient points to ensure that the trajectory is still completed.

Unfortunately, accounting for eclipse periods does significantly increase the computation time for each solution. What would have originally taken minutes to compute without eclipse periods now takes hours to compute while optimizing around them. This places the computation time on par with that of the more robust tools that do not account for eclipse periods in the optimization.

B. Optimizing Around Eclipses

To demonstrate how optimizing around eclipse periods improves the ability to minimize both the fuel use and time-of-flight for the transfer, an example scenario (in orbit about Earth) was run with the initial and final COEs seen in Table 4.

Figure 3 shows this example scenario (assuming a spacecraft mass of 2000 kg, a specific impulse I_{sp} of 3500 s, and a thrust of 0.30 N) for various efficiency thresholds. In Fig. 3, three scenarios are compared: no eclipse periods, optimized around eclipse periods, and including eclipse periods as unplanned outages. In examining the plots, the results are as expected for a method that successfully optimizes for eclipse periods. As seen in the plot, not optimizing around the included eclipses uses only slightly more propellant than including the eclipse periods as unplanned outages but takes much longer to complete the transfer for each given efficiency threshold. As the

Table 4 Initial and final COEs for the transfer scenario

Classic orbital element	Initial state	Desired final state
a, km	16,000	18,000
e	0.5	0.4
i, deg	0	5
Ω	100 deg	Free
ω	0 deg	Free

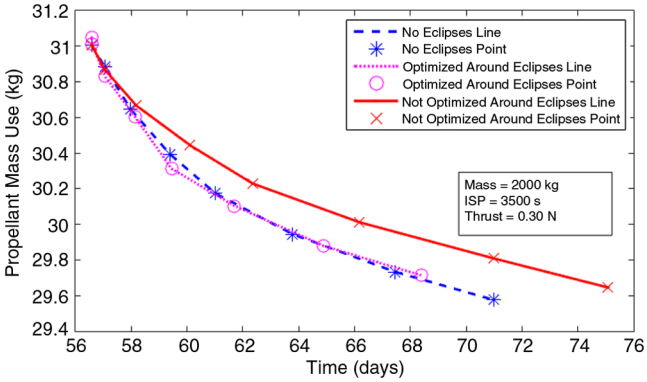

Fig. 3 Propellant mass consumption vs maneuver time at various efficiency thresholds.

efficiency threshold increases, the distance between the points on these two curves increases as well, where the difference between the maneuver times increase as the propellant consumption converges. Thinking about how the eclipses affect the mass/time curve, this makes sense. Simply not thrusting during eclipses means adding maneuver time but always thrusting when it is only the most efficient to do so, maintaining a low propellant mass use. When optimizing around the eclipse periods, because the efficiency threshold is compared to the new lower average efficiency value (as shown in Fig. 2), thrusting is now allowed at somewhat less efficient times. This means that more propellant will be used each revolution, but that is counteracted by the decrease in the total number of revolutions necessary to complete the maneuver, resulting in a slightly lower fuel mass use when optimizing around eclipse periods. As the efficiency threshold is increased, the amount of extra time spent thrusting increases, and so does the efficiency of the newly allowed thrusting region. With higher thrusting efficiencies, the propellant mass use approaches the mass use value for when not optimizing for the eclipse periods. The increased time spent thrusting each revolution decreases flight time compared to accounting for eclipse periods as unplanned shutoffs. The result is an overall higher propellant/time curve when not optimizing around eclipses, as reflected in Fig. 3. The differences in the two curves including eclipse periods demonstrates how optimizing around the eclipse periods improves the accuracy of the results compared to simply not thrusting during the eclipses.

Comparing the results to when eclipse periods are not included at all shows how beneficial it can be to optimize around eclipse periods. Because the eclipse occurs at perigee in this scenario (one of the most efficient points to thrust in the orbit), adding in the eclipse periods causes an overall increase in maneuver time and propellant. However, the two scenarios are almost identical for most of the curve because optimizing for eclipses allows for additional thrusting to help counteract the shutoffs, as is the goal of optimizing around eclipse periods. The fact that optimizing around eclipse periods yields a curve more similar to the no-eclipse curve than the curve where the eclipse period is accounted for as only an unplanned shutoff shows that optimizing the transfer and thrusting in different places can provide a similar result to the favorable, eclipse-free scenario.

C. Application

Now that the tool has been shown to produce a propellant mass consumption vs maneuver time curve while optimizing a trajectory with eclipse periods nearly equivalent to that as if the trajectory were solved without eclipse periods, the same optimization technique can be applied to a real solar electric-propulsion maneuver. The geostationary transfer orbit (GTO) to geostationary equatorial orbit (GEO) transfer is a highly researched maneuver in the astrodynamics community due to its complexity and potential for lucrative applications. Though the GTO-to-GEO transfer has yet to be attempted with a solar electric-propulsion satellite due to a large transfer time, interest in using such a maneuver is still strong. The GTO-to-GEO transfer (define in Table 5) was solved similar to the

Table 5 Initial and final COEs for the GTO-to-GEO transfer scenario

Classic orbital element	Initial state	Desired final state
a, km	24, 364	42, 164
e	0.7306	0
i, deg	27	0
Ω	280 deg	Free
ω	0 deg	Free

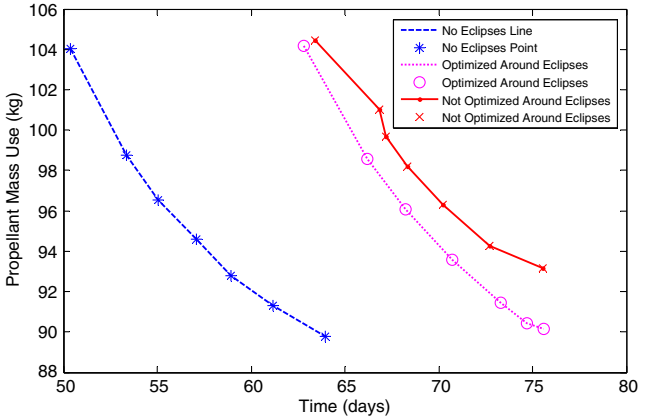

Fig. 4 Propellant mass consumption vs maneuver time for a GTO-to-GEO transfer.

preceding test case (with the mass decreased to 1500 kg and thrust increased to 1 N) except assuming that the initial orbit is oriented such that eclipses occur at apogee.

Solving again for the transfer scenario with no eclipses, optimizing the transfer around eclipse periods, and optimizing the transfer with eclipses included as unplanned outages, the curves produced (see Fig. 4) show how difficult it is to optimize such a maneuver around eclipse periods but that it can still be done with some success.

Although the curve when optimizing around eclipse periods does not align as well with the curve with no eclipse periods as in the earlier test case, the curve produced when optimizing around eclipse periods is still an improvement compared to accounting for eclipse periods as unplanned shutoffs. Given that optimization around eclipse periods can still be accomplished with such a complex maneuver suggests that the technique used will produce similar, if not better, results for almost any desired solar electric-propulsion orbit transfer.

IV. Conclusions

As the field of solar electric-propulsion maneuver optimization currently stands, missions are designed using various different techniques of solving for many-revolution, electric-propulsion trajectories that only allow for eclipses to be accounted for as unplanned shutoffs. Accounting for eclipse periods as only unplanned shutoffs, however, can require a significantly longer maneuver time than if the trajectory were optimized around the eclipse periods. Doing so allows for thrusting at slightly less efficient points in each revolution, thus significantly decreasing the required maneuver time, whereas the fuel use is maintained at nearly the same value. Although this technique can currently only optimize the transfer for each single revolution, this has only a minor effect on the extent to which both the fuel use and the time-of-flight can be minimized.

In optimizing a GTO-to-GEO transfer around eclipse periods, a complex orbit transfer was solved using this technique while saving a significant amount of flight time compared to methods currently used to design solar electric-propulsion maneuvers. The hope is that the results of this study will lead to similar techniques being employed in other, more robust tools used in trajectory design so that similar maneuver duration savings can be accomplished in future missions.

References

[1] Chobotov, V. A., *Orbital Mechanics*, 3rd ed., AIAA, Reston, VA, 2002, pp. 335–353.

[2] Conway, B. A., *Spacecraft Trajectory Optimization*, Cambridge Univ. Press, New York, 2010, pp. 139–177.

[3] Kluever, C. A., "Using Edelbaum's Method to Compute Low-Thrust Transfers with Earth-Shadow Eclipses," *Journal of Guidance, Control, and Dynamics*, Vol. 34, No. 1, 2011, pp. 300–303.

[4] Petropoulos, A., Tarzi, Z., Lantoine, G., Dargent, T., and Epenoy, R., "Techniques For Designing Many-Revolution Electric-Propulsion Trajectories," *Advances in the Astronautical Sciences*, Vol. 152, No. 3, Jan. 2014, pp. 2367–2386.

[5] Reiter, J. A., Nicholas, A. K., and Spencer, D. B., "Optimization of Many-Revolution, Electric-Propulsion Trajectories with Engine Shutoff Constraints," *Proceedings of the AAS/AIAA Space Flight Mechanics Meeting*, AAS Paper 15-237, Williamsburg, VA, Jan. 2015.

[6] Ruggiero, A., Pergola, P., Marcuccio, S., and Andrenucci, M., "Low-Thrust Maneuvers for the Efficient Correction of Orbital Elements," *Proceedings of the 32nd International Electric Propulsion Conference*, IEPC Paper 2011-102, Sept. 2011, pp. 1–13.

[7] Vallado, D. A., *Fundamentals of Astrodynamics and Applications*, 4th ed., Microcosm Press, Hawthorne, CA, 2013, pp. 299–302.

M. L. R. Walker
Associate Editor